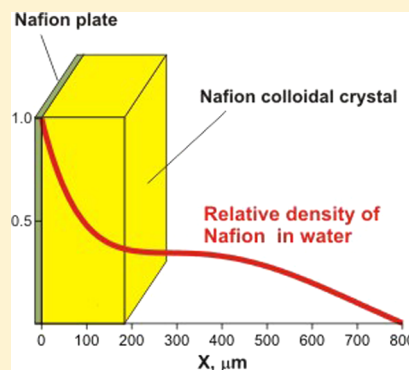


## Colloidal Crystal Formation at the “Nafion–Water” Interface

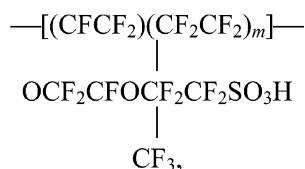
Nikolay F. Bunkin,<sup>\*,†,§,||</sup> Vladimir S. Gorelik,<sup>‡,§</sup> Valeriy A. Kozlov,<sup>†</sup> Alexey V. Shkirin,<sup>†</sup> and Nikolay V. Suyazov<sup>†</sup><sup>†</sup>A.M. Prokhorov General Physics Institute, Moscow, Vavilova 38, 119991 Russia<sup>‡</sup>P.N. Lebedev Physical Institute, Moscow, Leninskiy prospekt 53, 119991 Russia<sup>§</sup>Bauman Moscow State Technical University, Moscow, Second Baumanskaya, 5, 105005 Russia<sup>||</sup>Institute of Cell Biophysics, Pushchino, Moscow Region, Institutskaya 3, 142290 Russia

**ABSTRACT:** In our recent work [Bunkin et al. *Water* 2013, 4, 129–154] it was first obtained that the water layer, having a size of several tens of micrometers and being adjacent to the swollen Nafion interface, is characterized by enhanced optical density; the refractive index of water at the interface is 1.46. Furthermore, the birefringence effect was observed in this layer. To explain these results, it has been hypothesized that because of “disentangling” of charged polymer chains from the Nafion surface toward the bulk of water, a photonic crystal close to the surface is formed [Bunkin et al. *Water* 2013, 4, 129–154]. In this paper, we describe experiments with laser-stimulated luminescence from dry and swollen Nafion. It was shown in the experiment with dry Nafion that the apparatus function of our experimental setup (Green’s function) is well-described by a Gaussian profile. It was obtained that a highly concentrated colloidal suspension of Nafion particles with a steep spatial boundary is formed in the water layer adjacent to the interface. The volume density of the Nafion particles as a function of the distance from the Nafion interface was found. These findings can be considered indirect confirmation of the previously formulated photonic crystal hypothesis [Bunkin et al. *Water* 2013, 4, 129–154].



## 1. INTRODUCTION

At the present time the proton-exchange membrane Nafion developed by the DuPont Company is widely used in manufacturing low-temperature (<1000 °C) hydrogen fuel cells. Nafion is a sulfonated tetrafluoroethylene-based fluoropolymer-copolymer. Its unique ionic properties result from incorporating perfluorovinyl ether groups terminated with sulfonate groups onto a tetrafluoroethylene backbone.<sup>1</sup> Its chemical formula is the following:



where  $m$  is the number of side chains; protons located on the  $\text{SO}_3\text{H}$  (sulfonic acid) groups can “hop” from one acid site to another one. Our interest in research of such membranes is first caused by the fact that such a membrane in contact with water exhibits well-expressed hydrophilic properties.<sup>1</sup> Therefore, it is quite natural to expect that Nafion should have an influence upon the near-surface molecular layers of water. Furthermore, our interest in investigating such membranes is highly motivated by some peculiar features, which are revealed by water in the vicinity of the Nafion interface. Specifically, according to numerous experimental results obtained in the group of Prof. G.H. Pollack, University of Washington, it was

shown that near the “Nafion–polar liquid” interface the so-called “exclusion zone (EZ)” from the side of a liquid is formed<sup>2–10</sup> whose macroscopic characteristics essentially differ from those in the bulk of the liquid. Any colloid particles are effectively pushed out of the EZ; therefore, this area is referred to as the exclusion zone. The effective size of this area was determined as the distance between Nafion interface and the border of colloid particles suspension and was found with the help of an optical microscope. This technique revealed that for water the EZ radius is 200–220  $\mu\text{m}$ .<sup>3</sup> It is important that the scale of the EZ grows with time, and the rate of this growth essentially increases provided that the liquid sample is irradiated at a wavelength being absorbed by that liquid (see refs 2 and 3). Additionally, the results of measuring the spatial distribution of electrostatic potential inside the EZ for water and aqueous solutions of various salts are given:<sup>3,9</sup> it appeared that in this area the potential is negative and reaches values to  $-120$  mV; as the distance between the Nafion interface and the electrostatic potential probe increases, the absolute value of the potential decays steeply, approaching  $-20$  mV at a distance of about 50  $\mu\text{m}$  from the interface; as the distance increases, the modulus of the electrostatic potential keeps falling, but not so steeply, revealing crossover-like behavior. The absolute value of the

Received: October 10, 2013

Revised: January 15, 2014

Published: February 25, 2014

potential decreases with increasing distance from the Nafion interface and approaches the zero level at approximately 1000  $\mu\text{m}$  from the interface. In accordance with the results of ref 7, the effective size of the EZ falls when admixing salts (in particular, NaCl) in water. As was obtained in refs 2 and 5, immersing a Nafion plate in water results in a decrease of the equilibrium pH value from 7 to approximately 5.5; these measurements were carried out at the distance of about 1 cm from the interface. To evaluate the pH value at the micrometer scale in a very close vicinity of the interface, the authors of refs 2 and 5 used particles of a pH-sensitive dye; it was revealed that the dye particles leave the EZ just like colloid particles. This is why it appeared impossible to measure pH inside the EZ, while immediately behind the EZ the value of pH was less than three. Moreover, as was obtained in ref 5, the EZ exhibits a birefringence property. It is worth mentioning the results of ref 10, where a spatial temperature distribution in the EZ was studied with the help of a thermal imaging camera. As was shown in this experiment, the EZ temperature is less than the equilibrium temperature in the bulk of water far from the EZ, i.e., the system studied in the quoted works was not in equilibrium with respect to temperature. Finally, as was shown in refs 9 and 10, the light absorption band, centered at a wavelength of 270 nm, arises in the EZ; this experiment was performed in such a way that the opportunity to interpret the results just due to absorption of light in the bulk of Nafion was excluded. It appeared<sup>9</sup> that the absorptivity at the given wavelength grows at admixing of some additives, in particular, chlorides of alkaline metals.

It is worth noting here that the problem of the interaction of a surface having hydrophilic or hydrophobic properties with polar liquids is still beyond complete comprehension; see, for example, ref 11 and the references therein. Nonetheless, the conventional point of view concerning the hydrophilic hydration radius (i.e., the spatial scale, where it is possible to treat the molecular structure of water as an ordered one) implies that this size is about several tens of nanometers, although in some works (see, for example, refs 12–15) it was noted that the effective radius of the interaction of colloidal particles in water can exceed one micrometer.

Thus, we are faced with a challenging problem: how to combine the incompatible, i.e., how to explain a large EZ size together with a nanometer-scaled hydrophilic hydration radius? In connection to this, we recently carried out a phase microscopy experiment; the experimental setup employed by us was described in detail previously.<sup>16–18</sup> In the experiment, we investigated a Nafion membrane swollen in water; the results were collected in ref 19. It was first obtained in this study that the refractive index of water at the Nafion interface  $n = 1.46$  and falls to the level of  $n_0 = 1.33$  (ordinary water) at the distance  $X_0 \approx 40 \mu\text{m}$  from the interface (see Figure 13 in ref 19). Furthermore, the birefringence effect was observed in the crossed polarizers experiment in the water layer adjacent to the Nafion interface (see Figure 14 in ref 19); the size of this layer was also about 40  $\mu\text{m}$  from the Nafion border. To explain these results, it has been hypothesized that the charged polymer chains disentangle from the surface of Nafion toward the bulk of water, thus forming a colloidal crystal (see schematic diagram in Figure 15 in ref 19). The colloidal crystal hypothesis was formulated on the basis of the aforementioned effect of radiation absorption at a wavelength of 270 nm in the EZ.

This work is devoted to direct proof of the formation of a very concentrated aqueous solution of the Nafion particles in

the vicinity of the Nafion interface. The spatial boundary of the area, where this solution exists, is rather steep, and the area size corresponds to the EZ size.

## 2. EXPERIMENTAL SECTION

**2.1. Preparation of Samples.** In the experiments, specimens of Nafion manufactured by DuPont Company have been investigated; their thickness was 175  $\mu\text{m}$ . The water samples for the immersion of Nafion plates were of 5 M $\Omega$  cm resistivity with pH 5.5–5.8.

Below we describe the experiments of measuring UV-stimulated luminescence close to the Nafion interface (Figure 1). The probe radiation of the laser diode at a wavelength of

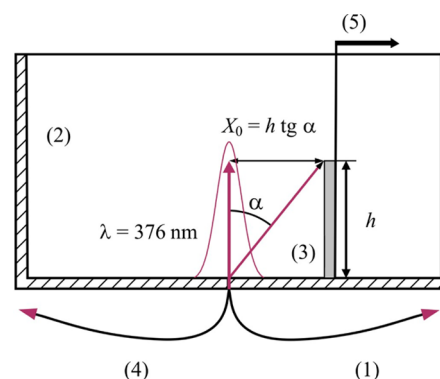


**Figure 1.** Schematic of the experimental setup for measuring the luminescence from dry Nafion: (1) multimode optical fiber of the incident probe radiation having a Gaussian intensity profile; (2) Teflon cell; (3) Nafion plate with height  $h$ ; (4) multimode optical fiber for receiving the luminescence signal; (5) table with micrometer pitch. Distance  $X_0$  sets the measurement error. In the case of measuring the luminescence from swollen Nafion, the cell (2) was filled with water and the cell was rotated by an angle  $\alpha > 6^\circ$  counterclockwise to avoid illuminating the Nafion plate (3) by the incident beam reflected from the water surface.

376 nm was put into a multimode optical fiber (we denote it as the incident probe radiation fiber (1) in Figure 1) with the following characteristics: the fiber core diameter was 50  $\mu\text{m}$ , i.e., one could assume that the diameter of the output optical beam (having a Gaussian intensity profile) at the fiber window was also 50  $\mu\text{m}$ . For the fiber used, the numerical aperture was 0.3, which corresponds to the maximum angle of the output beam divergence  $\alpha = 17^\circ$ . The probe fiber and an identical receiving fiber (the latter is denoted as (4) in Figure 1) were fixed in the hole, made in the center of the bottom of a cylindrical Teflon cell (2); thus, the optical axis coincides with the axis of the cell. A square plate of Nafion (3) with the height  $h = 4 \text{ mm}$  and the thickness of 175  $\mu\text{m}$  was mounted in the cell (2) parallel to the optical axis, and the probe beam irradiated the Nafion plate interface in grazing incidence geometry. When we explored the samples of dry Nafion, the cell (2) was empty, while in the case of investigating the samples of swollen in water Nafion the cell was filled with water. The output window of the fiber (1) was aligned with the lower boundary of the Nafion plate (see Figure 1); bearing in mind the geometry of the experiment, the near-field approximation was fulfilled, and the diffraction effects can be ignored. Radiation at the wavelength of 376 nm stimulated luminescence from Nafion in the spectral range from 460 to 650 nm; this radiation was received by the multimode optical fiber (4), having the same characteristics as fiber (1), and then

was input to a mini-spectrometer (not shown in Figure 1). Diffuse scattering of the luminescent light by the Teflon walls leads to an effective growth of the luminescence volume, i.e., to an increase of the luminescence signal at the fiber (4) input window. The Nafion plate was fixed on a table (5) with horizontal micrometer pitch, having a step of  $25\ \mu\text{m}$ ; special attention was paid to avoiding folds and wrinkles on the plate surface, i.e., it was important to ensure that the surface was as smooth as possible and oriented parallel to the optical axis. The micrometer screw was rotated in one direction (to avoid spring hysteresis effects), and the Nafion plate moved away from the optical axis. In this experiment, we investigated the spectra of luminescence from dry and swollen in water Nafion (we soaked the Nafion plate for 5 h) as the function of distance  $X$  between the optical axis and the Nafion interface. The point of origin ( $X = 0$ ) was determined from the requirement of maximum luminescence that corresponds to such relative orientation of the probe beam and the Nafion plate when the plate is located exactly along the central part of the beam having a Gaussian intensity profile. Because the height  $h$  of the plate along the optical axis was 4 mm and a maximum angle of divergence of the incident probe radiation  $\alpha = 17^\circ$ , the radius of the light cone with height  $h$  is expressed as  $X_0 = h \tan \alpha = 1200\ \mu\text{m}$  (Figure 1). Scale  $X_0$  is the maximum distance where the probe radiation can still stimulate luminescence from Nafion. In the experiments with dry Nafion, we actually define the experimental error, which is basically controlled by the divergence of the incident beam, by irregularities of the plate surface and by the fact that this surface was not strictly parallel to the optical axis. Note that in the experiments with the swollen Nafion, i.e., when the cell (2) was filled with water, it was very important to avoid illuminating the Nafion interface by the incident radiation reflected from the water surface. For this purpose, the optical axis of the system was turned to an angle  $\alpha > 17^\circ$  relative to the horizontal plane in such a way that all incident radiation was reflected from the water surface to the opposite (with respect to the Nafion interface) direction. Finally, we verified that in the absence of Nafion, any luminescence from the water in this spectral range was absent.

The spectra of the luminescence from dry and swollen Nafion are shown in panels a and b of Figure 2, respectively. Each spectrogram was taken after shifting the Nafion plate for a distance of  $25\ \mu\text{m}$  from the optical axis: in both graphs the upper spectrogram is related to a situation where the central part of the incident beam coincides with the Nafion interface, which corresponds to  $X = 0$ . As follows from the graphs, the spectra of luminescence from dry and swollen Nafion are absolutely identical. The maximum of luminescence in both cases is related to a wavelength  $\lambda = 508\ \text{nm}$ . Figure 3 shows the dependence of the luminescence intensity at this wavelength as a function of the distance  $X$  between the Nafion interface and the optical axis for dry and swollen Nafion. As is seen from Figure 3, in the case of dry Nafion, the luminescence completely decays at the distance  $X_1 \approx 125\ \mu\text{m}$ ,  $X_1 < X_0 = 1200\ \mu\text{m}$ , and in the case of swollen Nafion, the luminescence decays at  $X_2 \approx 750\ \mu\text{m}$ . Thus,  $X_{1,2} < X_0 = 1200\ \mu\text{m}$ , i.e., the values  $X_1$  and  $X_2$  are within the maximum distance between the optical axis and the Nafion interface.

However, as we show below, the real accuracy of our measurements coupled to Gaussian probe beam divergence is  $84\ \mu\text{m}$ . In our view, the graph in Figure 3 can be interpreted as evidence for the existence of a transition layer between water and the swollen polymer. We can imagine this layer to be an

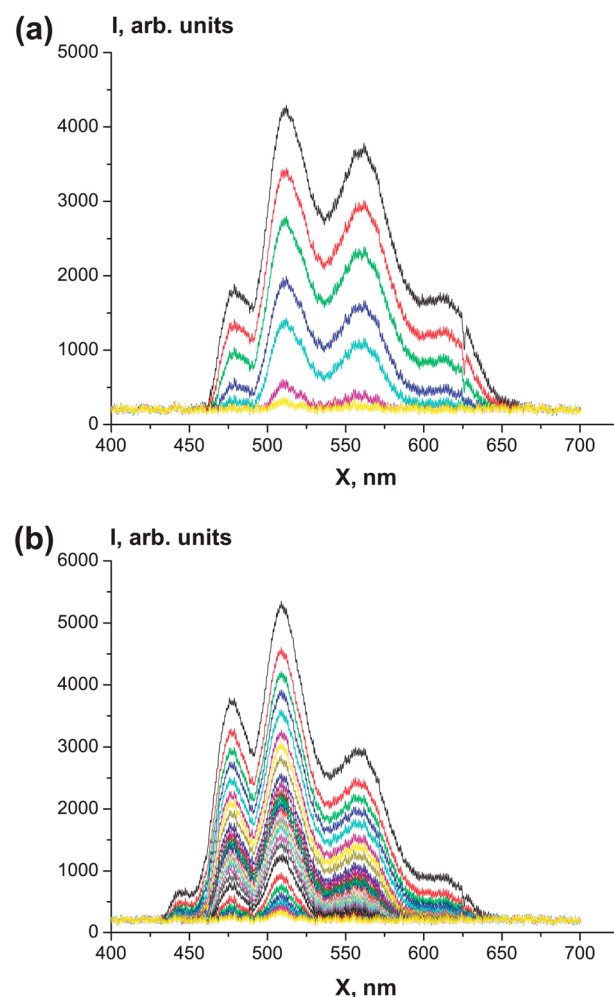


**Figure 2.** Luminescence spectra from dry (a) and swollen (b) Nafion. The shift between the successive spectrograms corresponds to the displacement of the Nafion plate for the distance  $X = 25\ \mu\text{m}$  from the optical axis. Uppermost spectrograms correspond to the case where  $X = 0$ .

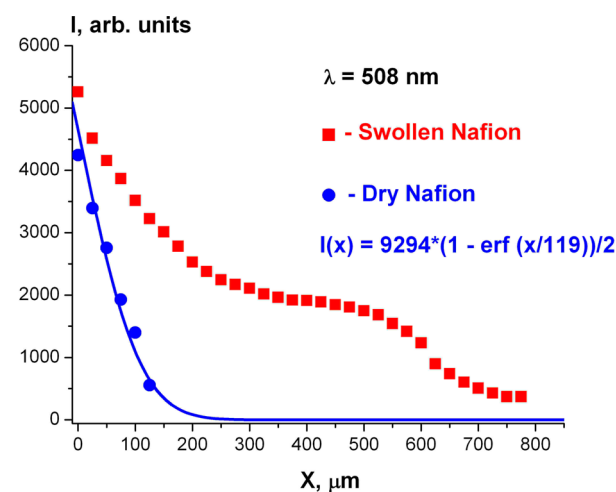


**Figure 3.** Intensity of luminescence (in arbitrary units) from dry (blue circles) and swollen (red squares) Nafion at the wavelength 508 nm vs the distance between the Nafion interface and the optical axis. Blue solid curve is the theoretical approximation of the luminescence intensity from dry Nafion (see Discussion).



aqueous solution of Nafion with a very high concentration. It is important that this layer has a distinct spatial boundary, and the gradient of Nafion concentration should arise at this boundary. At the same time, at equilibrium, any concentration gradients cannot exist. Thus, we deal with a very specific state of aqueous solution of Nafion.

### 3. DISCUSSION

Let us denote  $\rho(x)$  as the linear (scaled in kilograms per meter) density of the Nafion particles, i.e., it is the Nafion content in a planar layer of a unit thickness; this layer is separated from the Nafion interface by the distance  $x$  and is oriented in parallel to this interface. The Nafion is transparent for the radiation employed in our experiment, and the luminescence intensity  $I(x)$ , detected at the distance  $x$  from the interface, is linearly dependent on the density distribution  $\rho(x)$ . Thus, for a sufficiently large longitudinal size of the cell (see (2) in Figure 1), along the  $X$ -axis the value of  $I(x)$  can be written as

$$I(x) = \int_{-\infty}^{\infty} G(x - x_1) \cdot \rho(x_1) dx_1 \quad (1)$$

The kernel operator  $G(x)$  (Green's function) is controlled by the apparatus function of the optical setup and the cell geometry along the direction normal to the  $X$ -axis. Bearing in mind that the probe radiation (1) in the multimode fiber has a Gaussian profile, Green's function can be simulated by the function  $G(x) = G_0 \exp[-x^2/2a^2]^{1/2}$ . In the case of dry Nafion, the density  $\rho(x)$  can be written as  $\rho(x) = \rho_0 \cdot \theta(-x)$ , where  $\theta(x)$  is the Heaviside function (the unit step function) and  $\rho_0$  is a constant of certain dimension. Equation 1 gives that for the chosen function  $G(x)$  the luminescence intensity  $I(x)$  for dry Nafion can be expressed by the error function

$$I(x) = G_0 \rho_0 a \sqrt{\frac{\pi}{2}} \left[ 1 - \operatorname{erf} \left( \frac{x}{\sqrt{2}a} \right) \right] \quad (2)$$

where  $G_0$  is another dimension constant and the value of parameter  $a$  can be determined from the experimental data; the graph of this function is illustrated by solid blue line in Figure 3. As is seen, the coincidence between the experimental points (blue circles) and the theoretic curve is quite satisfactory for  $a \approx 84 \mu\text{m}$ , which exceeds the diameter of the multimode fiber core in our setup less than two times, i.e., the estimated value of the parameter  $a$  looks reasonable. Summarizing, in the experiment with the luminescence from dry Nafion, we had an opportunity to determine the Green's function  $G(x)$  with high accuracy. Let us further assume that a particular solution to the distribution  $\rho(x)$  of the linear Nafion density in water (now we speak about the swollen Nafion) has the form

$$\rho(x) = Q_3(x) \cdot \theta(-x) + Q_3(x) \cdot \exp(-x/b) \quad (3)$$

where  $Q_3(x)$  is a third-degree polynomial. The free parameter  $b$  in eq 3 and the four coefficients of the polynomial  $Q_3(x)$  are determined from the requirement of best conformity between the experimental points (blue squares) and the theoretical curve (blue solid line) for the luminescence intensity  $I(x)$  (Figure 4); here the theoretical curve is given by eq 1, where the integrand  $\rho(x)$  is now expressed by eq 3 and the kernel operator  $G(x)$  is the Gaussian function (eq 2). The theoretical plot coincides with the experimental points within the whole area of  $x$ , i.e., we can speak about good accuracy of approximation (eq 3). The Nafion linear density  $\rho(x)$  is

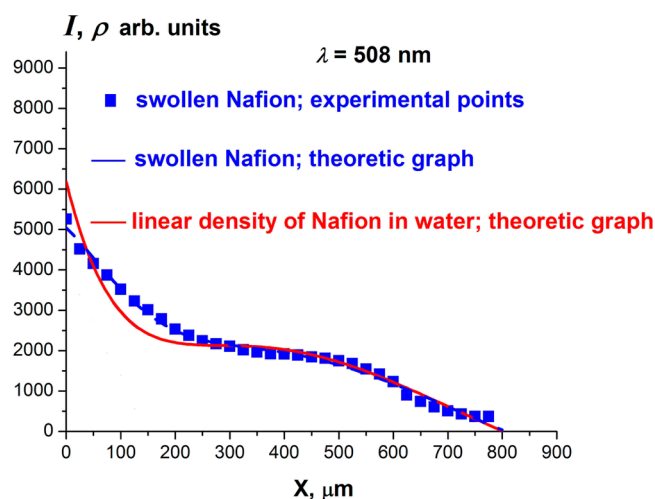


**Figure 4.** Intensity of luminescence  $I(x)$  (in arbitrary units) from the swollen (blue circles) Nafion at the wavelength 508 nm vs the distance  $x$  between the Nafion interface and the optical axis. Blue solid curve is the theoretic approximation of the experimental points. Red solid line is the distribution of linear density  $\rho(x)$  of Nafion in water, given by eq 3.

shown in Figure 4 by the red solid curve; the Heaviside function  $\theta(-x)$  is not revealed at the chosen scale of the abscissa axis.

As follows from the density graph  $\rho(x)$ , the gradient of  $\rho(x)$  is clearly seen in the area  $0 \leq x \leq 200 \mu\text{m}$ . In the area  $200 \leq x \leq 500 \mu\text{m}$  we can see a broad plateau; note that the Nafion density is still not zero within this area. Finally, for  $x > 500 \mu\text{m}$ , the linear Nafion density  $\rho(x)$  smoothly (without a pronounced gradient) tends to zero. It is important to note that eq 1 is related to the class of Fredholm integral equations of the first kind.<sup>20</sup> It is known that such equations have a unique solution, but this solution is unstable with respect to small deviations of the right-hand member of the equation, i.e., the function  $I(x)$ , which is the result of our measurements. In other words, the problem of finding a solution to this equation is the so-called ill-defined problem. Thus, the question of conformity between the theoretical solution  $\rho(x)$  and the real distribution of the Nafion density in water inevitably arises. It is very important for us that, according to the results of study,<sup>3</sup> the EZ size is approximately equal to 200–220  $\mu\text{m}$ . It is straightforward to assume that the EZ is just a concentrated solution of the Nafion particles with sharp spatial boundary, which must have a pronounced gradient of the Nafion density; in the framework of this assumption, we can claim that the theoretical function  $\rho(x)$  has a physical meaning.

Furthermore, as was shown in ref 21, the rodlike Nafion particles, which are negatively charged because of the presence of  $\text{R-SO}_3^-$  groups, are formed in the process of swelling Nafion in water. Thus, it is natural to assume that the Nafion particles in the EZ area ( $0 \leq x \leq 200 \mu\text{m}$ ) and the negatively charged rods, predicted in ref 21 are the same particles. However, the concentration gradient of any particles in a liquid under the equilibrium conditions can only exist provided that these particles are basically immobile (here we of course do not speak about two-component systems with limited miscibility, which can stratify in the gravity field). At the same time, Earnshaw's theorem in its general form<sup>22,23</sup> claims that charged immobile particles cannot be in stable static equilibrium under the influence of electrostatic forces alone. Thus, we should

suppose that certain nonelectrostatic forces must be involved in our system. In our opinion, such forces are the intermolecular attraction forces, which are obviously caused by the covalent bonds; these forces keep the negative Nafion rodlike particles anchored to the negatively charged Nafion interface, i.e., such negatively charged rods are strongly bound with the Nafion interface and cannot be completely torn off that interface. Thus, the rodlike particles are subjected to the repulsive Coulomb force from the interface, being oriented normally to the interface and parallel to one another. An additional argument in favor of this model is that the grazing incidence small-angle X-ray scattering and atomic force microscopy experiments with Nafion swollen in water<sup>24</sup> show that the bundles of such rodlike particles are oriented predominantly normal to the water–Nafion interface (in contrast to the case in which Nafion contacts water vapor; in this case, the rodlike particles are oriented along the interface).

Within the framework of this model, we can explain (still at a qualitative level) the rise of the refractive index in the EZ, which was first observed in our previous study.<sup>19</sup> Indeed, according to our data (see Figure 13 in ref 19), the refractive index is 1.46 at the Nafion–water interface, while for the ordinary water  $n_0 = 1.33$ . If there were no effect of the preferential orientation of the rodlike particles normal to the Nafion interface, the increase of the refractive index would reveal itself only in a very thin surface layer (thickness of this layer should be of the order of a few monolayers), and we just could not measure the refractive index in the layer of such thickness because the spatial resolution of our experimental setup described in study<sup>19</sup> was controlled by the size of the laser spot (about 1  $\mu\text{m}$ ).

Let us properly consider not the refractive index  $n$  but the so-called molecular refraction  $\gamma = (n^2 - 1)/(n^2 + 2)$  (see refs 25 and 26), which is given by

$$\gamma = \frac{4\pi}{3} N\alpha \quad (4)$$

where  $\alpha$  is the electronic polarizability of molecules and  $N$  is their specific density (their number per volume unit). Our refraction measurements in the vicinity of Nafion indicate<sup>19</sup> that the molecular refraction  $\gamma$  rises by about 30% compared to that of the bulk of water. Let us first examine the possibility of the refraction growth because of increasing the electronic polarizability  $\alpha$  of water molecules. The value of  $\alpha$  can rise because of their orientation ordering. At the same time, the maximum excess of the polarizability relative to its mean value  $\bar{\alpha}$  (the polarizability at a random orientation of molecules) can be expressed as  $(\alpha_{\text{max}} - \bar{\alpha})/\bar{\alpha}$ ; for water (see ref 27),  $\bar{\alpha} = 1.47 \times 10^{-24} \text{ cm}^3$  and  $\alpha_{\text{max}} = 1.66 \times 10^{-24} \text{ cm}^3$ , i.e.,  $(\alpha_{\text{max}} - \bar{\alpha})/\bar{\alpha} \approx 0.13$ ; this is the upper estimate because such polarizability increase is possible only at the total orientation ordering of all molecules. This is why the polarizability growth cannot explain the 30% increase of the molecular refraction. Thus, the only mechanism responsible for the refraction growth is the increase of  $N$ . As was shown in ref 28, the water density can be enhanced essentially within the protein hydration shell. The results<sup>28</sup> point to the existence of the first hydration shell with the average water density approximately 10% higher than that of the bulk water; note that protein is essentially hydrophilic, just the same as Nafion. We can imagine that the dipolar water molecules are attracted to the negatively charged rods, giving rise to the effective growth of the molecular density  $N$  in the EZ.

It is important that the spatial configuration of the like-charged rods in the EZ can be stable, provided only that the mean distance between two arbitrary neighboring rodlike particles should be equal (indicating the absence of the Coulomb force gradients), i.e., these particles are to be packed with a certain order, similar to that of the colloidal crystal structure, formed by charged Polystyrene microspheres in water (see, e.g., refs 29–32). In the framework of this colloidal crystal model, the effect of birefringence in the EZ, which was first observed in ref 5 and then was confirmed in our work,<sup>19</sup> finds its natural explanation. Indeed, we deal with a distinct anisotropy of our system due to the presence of the preferential direction along the normal to the Nafion interface. Note that the liquid-crystalline model of the EZ was developed earlier in refs 2–10 and was based upon assumption of the ordered arrangement of water molecules in this area. According to the quoted studies, the water molecules in the EZ can form dipolar domains because of the hydrophilic surface effect, and the radius of spatial correlation of these domains amounts to a few hundred or even thousands of micrometers. We do not argue with this viewpoint: in some cases, water molecules can form long-correlated crystalline phase. In our opinion, this water crystalline structure should be somehow stabilized; the negatively charged and highly hydrophilic rodlike Nafion particles having the spatially periodic arrangement can provide such stabilization. Assuming that the length of these rodlike particles can be about 100–200  $\mu\text{m}$ , such stabilization looks quite possible. Note that this hypothesis does not contradict the known fact<sup>11</sup> that the hydrophilic substrate can modify the properties of adjacent water within only 1–2 monolayers, i.e., at the scale of several nanometers. Order parameter of the colloidal crystal formed by the Nafion rods can be introduced by analogy with liquid crystals (see, e.g., refs 33 and 34) in the form  $S(x) = \langle 3 \cos^2 \theta - 1/2 \rangle$ , where  $x$  is the distance from the Nafion interface and  $\theta$  is the angle between the normal to the interface (polar axis in spherical coordinates) and the axis of a charged rod. Here the angle brackets mean averaging in spherical coordinates for all charged rods. We assume that at  $x = 0$  we deal with an ideal orientation of the rods along the polar axis, i.e.,  $\theta = 0$  or  $180^\circ$ , and  $S(0) = 1$ , whereas behind the EZ, i.e., for  $x > x_0 = 200 \mu\text{m}$ , a state of complete disorder is realized and  $S(x > x_0) = 0$ . A more detailed theoretical description of the colloid crystal in terms of the order parameter will be published elsewhere.

The natural question arises: what is the state of the Nafion solution behind the gradient area, i.e., within the plateau extending from 200 to 500  $\mu\text{m}$ ? Obviously, the characteristic size of this plateau does not allow us to couple it with the EZ. We still do not have any interpretation of the origin of the plateau. Our preliminary results indicate that this region corresponds to a highly viscous aqueous suspension of the charged particles of Nafion, i.e., we probably deal with very slow dissolution of Nafion in water. Currently, we carry out the experiments with varying times of Nafion soaking and measure the size of this plateau. But at the moment, the question of the nature of this plateau is open.

The question of the Coulomb stability of the spatial structure consisting of negatively charged rodlike Nafion particles in the EZ should be analyzed separately. It is clear that the arrangement of such particles is controlled by spatial distribution of the electrostatic field generated by the charged surfaces; if (as was the case in the experiments with the luminescence excitation) we deal with elongated planar Nafion

interface, the electrostatic field is rather homogeneous (at least far from the edges of a Nafion plate). At the same time, if Nafion contacts water within a narrow strip (as was the case in our refractometry and birefringence experiments,<sup>19</sup> where the thickness of Nafion spacer was only 175  $\mu\text{m}$ ), the electrostatic field cannot anymore be considered to be a homogeneous field. Probably this is the reason for the difference in the spatial scales found in those experiments: several hundred micrometers in the luminescence experiments and several tens of micrometers in the refractometry and birefringence experiments.

## AUTHOR INFORMATION

### Corresponding Author

\*E-mail: nbunkin@kapella.gpi.ru.

### Notes

The authors declare no competing financial interest.

## ACKNOWLEDGMENTS

The authors are indebted to Prof. G.H. Pollack for his permanent interest to our work and very fruitful discussions of the results. This study was supported in part by the Russian Foundation for Basic Researches, Grant 13-02-00731 A, and Presidium of Russian academy of sciences Program 28, "The origin of life and the formation of the biosphere" (subprogram I, the subject "Physics, Chemistry and Biology of Water") and the RCSF Grant 14-12-00734.

## REFERENCES

- (1) Mauritz, K. A.; Moore, R. B. State of Understanding of Nafion. *Chem. Rev.* **2004**, *104*, 4535–4586.
- (2) Chai, B.; Yoo, H.; Pollack, G. H. Effect of Radiant Energy on Near-Surface Water. *J. Phys. Chem. B* **2009**, *113*, 13953–13958.
- (3) Chai, B.; Pollack, G. H. Solute-Free Interfacial Zones in Polar Liquids. *J. Phys. Chem. B* **2010**, *114*, 5371–5375.
- (4) Bhalerao, A. S.; Pollack, G. H. Light-induced effects on Brownian displacements. *J. Biophotonics* **2011**, *4*, 172–177.
- (5) Yoo, H.; Baker, D. R.; Pirie, C. M.; Hovakeemian, B.; Pollack, G. H. Characteristics of Water Adjacent to Hydrophilic Interfaces. In *Water: The Forgotten Biological Molecule*; Le Bihan, D., Fukuyama, H., Eds.; Pan Stanford Publishing: Singapore, 2011; pp123–138.
- (6) Yoo, H.; Paranj, R.; Pollack, G. H. Impact of Hydrophilic Surfaces on Interfacial Water Dynamics Probed with NMR Spectroscopy. *J. Phys. Chem. Lett.* **2011**, *2*, 532–536.
- (7) Zhao, Q.; Coult, J.; Pollack, G. H. Long-range attraction in aqueous colloidal suspensions. *Proc. SPIE* **2010**, 7376, 73761C-1–73761C-13.
- (8) Zheng, J.; Pollack, G. H. Long-range Forces Extending from Polymer-gel Surfaces. *Phys. Rev. E* **2003**, *68* (031408), 1–7.
- (9) Chai, B.; Zheng, J.; Zhao, Q.; Pollack, G. H. Spectroscopic Studies of Solutes in Aqueous Solution. *J. Phys. Chem. A* **2008**, *112*, 2242–2247.
- (10) Zheng, J.; Chin, W. C.; Khijniak, E.; Khijniak, E., Jr.; Pollack, G. H. Surfaces and Interfacial Water: Evidence that Hydrophilic Surfaces Have Long-range Impact. *Adv. Colloid Interface Sci.* **2006**, *127*, 19–27.
- (11) Ninham, B. W.; Lo Nostro, P. *Intermolecular Forces and Self Assembly: In Colloid, Nano Sciences and Biology*; Cambridge University Press: New York, 2010.
- (12) Kepler, G. M.; Fraden, S. Attractive Potential Between Confined Colloids at Low Ionic-Strength. *Phys. Rev. Lett.* **1994**, *73*, 356–359.
- (13) Crocker, J. C.; Grier, D. G. When Like Charges Attract: The Effects of Geometrical Confinement on Long-Range Colloidal Interactions. *Phys. Rev. Lett.* **1996**, *77*, 1897–1900.
- (14) Xu, X. H.; Yeung, E. S. Long-range Electrostatic Trapping of Single Protein Molecules at a Liquid/Solid Interface. *Science* **1998**, *281*, 1650–1653.
- (15) Squires, T. M.; Brenner, M. P. Like-Charge Attraction and Hydrodynamic Interaction. *Phys. Rev. Lett.* **2000**, *85*, 4976–4976.
- (16) Bunkin, N. F.; Suyazov, N. V.; Shkirin, A. V.; Ignatiev, P. S.; Indukaev, K. V. Nanoscale Structure of Dissolved Air Bubbles in Water as Studied by Measuring the Elements of the Scattering Matrix. *J. Chem. Phys.* **2009**, *130* (134308), 1–13.
- (17) Bunkin, N. F.; Suyazov, N. V.; Shkirin, A. V.; Ignatiev, P. S.; Indukaev, K. V. Cluster Structure of Stable Dissolved Gas Nanobubbles in Highly Purified Water. *J. Exp. Theor. Phys.* **2009**, *108*, 800–816.
- (18) Bunkin, N. F.; Ninham, B. W.; Shkirin, A. V.; Ignatiev, P. S.; Kozlov, V. A.; Starosvetskij, A. V. Long-living Nanobubbles of Dissolved Gas in Aqueous Solutions of Salts and Erythrocyte Suspensions. *J. Biophotonics* **2011**, *4*, 150–164.
- (19) Bunkin, N. F.; Ignatiev, P. S.; Kozlov, V. A.; Shkirin, A. V.; Zakharov, S. D.; Zinchenko, A. A. Study of the Phase States of Water Close to Nafion Interface. *Water* **2013**, *4*, 129–154.
- (20) Bitsadze, A. V. *Integral Equations of First Kind*; World Scientific Publishing Co. Pte. Ltd.: Singapore, 1995.
- (21) Gebel, G. Structural Evolution of Water Swollen Perfluor-sulfonated Ionomers from Dry Membrane to Solution. *Polymer* **2000**, *41*, 5829–5838.
- (22) Laud, B. B. *Electromagnetics*; New Age International (P) Ltd.: New Delhi, 1987; p 65.
- (23) Jones, W. Earnshaw's theorem and the stability of matter. *Eur. J. Phys.* **1980**, *1*, 85–88.
- (24) Bass, M.; Berman, A.; Singh, A.; Konovalov, O.; Freger, V. Surface-Induced Micelle Orientation in Nafion Films. *Macromolecules* **2011**, *44*, 2893–2899.
- (25) Lorentz, H. A. *The Theory of Electrons and its Applications to the Phenomena of Light and Radiant Heat*; B. G. Teubner: Leipzig, Germany, 1916.
- (26) Born, H.; Wolf, E. *Principles of Optics*; Pergamon Press: Oxford, U.K., 1964.
- (27) Wuks, M. F. *Electrical and Optical Properties of Molecules and Condensed Media*; LSU: Leningrad, Russia, 1984.
- (28) Svergun, D. I.; Richard, S.; Koch, M. H. J.; Sayers, Z.; Kuprin, S.; Zaccai, G. Protein Hydration in Solution: Experimental Observation by X-ray and Neutron Scattering. *Proc. Natl. Acad. Sci. U.S.A.* **1998**, *95*, 2267–2272.
- (29) Van Winkle, D. H.; Murray, C. A. Layering Transitions in Colloidal Crystals as Observed by Diffraction and Direct-Lattice Imaging. *Phys. Rev. A* **1986**, *34*, 562–573.
- (30) Van Winkle, D. H.; Murray, C. A. Experimental Observation of Two-Stage Melting in a Classical Two-Dimensional Screened Coulomb System. *Phys. Rev. Lett.* **1987**, *58*, 1200–1203.
- (31) Van Winkle, D. H.; Murray, C. A. Layering in Colloidal Fluids Near a Smooth Repulsive Wall. *J. Chem. Phys.* **1988**, *89*, 3885–3892.
- (32) Aastuen, D. J. V.; Clark, N. A.; Cotter, L. K.; Ackerson, B. J. Nucleation and Growth of Colloidal Crystals. *Phys. Rev. Lett.* **1986**, *57*, 1733–1736.
- (33) Chandrasekhar, S. *Liquid Crystals*, 2nd ed.; Cambridge University Press: Cambridge, U.K., 1992.
- (34) Collings, P. J.; Hird, M. *Introduction to Liquid Crystals*; Taylor & Francis: Philadelphia, PA, 1997.